Mutational analysis identifies residues crucial for homodimerization of Myeloid Differentiation Factor 88 (MyD88) and for its function in immune cells

Maria Loiarro [1,2], Elisabetta Volpe[3], Vito Ruggiero[4], Grazia Gallo[4], Roberto Furlan[5], Chiara Maiorino[5], Luca Battistini[3], and Claudio Sette[1,2]

[1]From the Department of Biomedicine and Prevention, University of Rome "Tor Vergata", 00133 Rome, Italy, [2]Laboratory of Neuroembryology and [3]Laboratory of Neuroimmunology, Santa Lucia Foundation, 00143 Rome, Italy, the [4]R&D Sigma-Tau S.p.A., 00040 Pomezia (RM), Italy and the [5]INSPE, Division of Neuroscience, San Raffaele Scientific Institute, 20132 Milan, Italy

*Running title: MyD88 dimerization and function in immune cells

To whom correspondence should be addressed: Prof. Claudio Sette, Department of Biomedicine and Prevention, University of Rome "Tor Vergata", 00133 Rome, Italy. Tel +39-06-72596260; Fax +39-06-72596268; E-mail: claudio.sette@uniroma2.it

Keywords: Immune response; TLR/IL-1R; MyD88; mutagenesis; NF-κB

The abbreviations used are: Myeloid differentiation factor 88, (MyD88); Toll-like receptor, (TLR); Inteleukin-1 receptor, (IL-1R); pathogen-associated molecular patterns, (PAMPs); lipopolysaccharide, (LPS); Toll/IL-1 receptor, (TIR); Death domain, (DD); Intermediate domain, (ID); IL-1 receptor-associated kinases, (IRAKs); IL-1R accessory protein, (IL-1RAcP); IL-1 receptor antagonist, (IL-1Ra); green fluorescent protein, (GFP); Nuclear factor κB, (NF-κB); Activator protein 1, (AP-1); Interferon-regulatory factors, (IRFs); Mitogen activated protein kinases, (MAPKs); Extracellular signal-regulated kinases, (Erks); Tumor necrosis factor-alpha, (TNF-α); Monocyte derived dendritic cells, (MDDCs).

Capsule

Background: MyD88 is an adaptor protein that plays a crucial role in the immune response.

Results: We identified residues within the TIR domain of MyD88 required for protein self-association.

Conclusion: Interference with the surface of homodimerization identified by these residues inhibits MyD88 function.

Significance: The inhibition of MyD88 activity could be a good therapeutic strategy for inflammatory and autoimmune diseases.

Abstract

Myeloid differentiation factor 88 (MyD88) is an adaptor protein that transduces intracellular signaling pathways evoked by the Toll-like receptors (TLRs) and interleukin-1 receptors (IL-1Rs). MyD88 is composed of an amino terminal Death domain (DD) and a carboxyl-terminal Toll/IL1 receptor (TIR) domain, separated by a short region. Upon ligand binding, TLR/IL-1Rs hetero- or homodimerize and recruit MyD88 through their respective TIR domains. Then, MyD88 oligomerizes via its DD and TIR domain and interacts with the interleukin-1 receptor-associated kinases (IRAKs) to form the Myddosome complex. We performed site-directed mutagenesis of conserved residues that are located in exposed regions of the MyD88-TIR domain, and analyzed the effect of the mutations on MyD88 signaling. Our studies revealed that mutation of Glu^{183}, Ser^{244} and Arg^{288} impaired homodimerization of the MyD88-TIR domain, recruitment of IRAKs and activation of NF-κB. Moreover, overexpression of two green fluorescent protein (GFP)-tagged MyD88 mini-proteins (GFP-$MyD88_{151-189}$ and GFP-$MyD88_{168-189}$), comprising the Glu^{183} residue, recapitulated these effects. Importantly expression of these dominant-negative MyD88 mini-proteins competed with the function of endogenous MyD88 and interfered with TLR2/4-mediated responses in a human monocytic cell line (THP-1) and in human primary monocyte derived dendritic cells (MDDCs). Thus, our studies identify novel residues of the TIR domain that are crucially involved in MyD88 homodimerization and TLR signaling in immune cells.

Introduction

All living organisms counteract the invasion of pathogens by setting up an innate immune response mediated by members of the superfamily of the Toll like- and interleukin-1-like receptors (TLR/IL-1R) (1,2) and by adaptor proteins that link them to downstream molecules involved in signaling pathways (3,4). To date 10 human TLRs (TLR1-10) and 12 murine TLRs (TLR1-9, TLR11-13) have been identified (5). TLRs detect different pathogen-associated molecular patterns (PAMPs) such as lipopeptides (TLR2), lipopolysaccharide (LPS) (TLR4), flagellin (TLR5), bacterial DNA (TLR9), and viral double- or single-stranded RNAs (TLR3 and TLR7/8, respectively) (6). TLRs are type I transmembrane proteins and comprise an extracellular domain, which mediates the recognition of PAMPs, a transmembrane region, and an intracellular Toll-IL-1 receptor (TIR) domain that activates downstream signaling pathways (5). Members of IL-1R family are characterized by the presence of extracellular immunoglobulin-like (Ig) domains and by an intracellular TIR domain (2,3). The prototype of these receptors is IL-1RI, which heterodimerizes with the homologous IL-1R accessory protein (IL-1RAcP) to form a receptor complex for the IL-1α, IL-1β and IL-1 receptor antagonist (IL-1Ra) proteins (2,3).

The adaptor protein family comprises 5 members, including the Myeloid differentiation factor 88 (MyD88) (4). MyD88 was first shown to be essential for IL-1 and IL-18 signaling (7) and, subsequently, for signaling of most TLRs (4,8,9). MyD88 has a modular structure with a Death domain (DD) at the N-terminus, an intermediate linker domain (ID) and a TIR domain at the C-terminus (10). The DD presents a fold that resembles a Greek key bundle of six antiparallel α-helices (11) and allows MyD88 oligomerization and its interaction with the respective DDs of the serine-threonine kinases IRAK1/2/4, thus resulting in a multimeric complex named Myddosome (12,13). This complex propagates the signal and leads to activation of transcription factors, such as the nuclear factor κB (NF-κB), the activator protein 1 (AP-1), and the interferon-regulatory factors (IRFs), and of mitogen activated protein kinases (MAPKs), such as the stress kinase p38 and the extracellular signal-regulated kinases 1 and 2 (ERK1/2) (14). The ID is a short region involved with the DD in the interaction of MyD88 with IRAK4 (15). The TIR domain displays a globular form, consisting of 5 β-sheets (βA-βE) and 4 α-helices (αA-αC and αE), connected to the β-strands by surface-exposed loops (16). The structure of the TIR domain of MyD88 is similar to that of other TLR/IL-1R superfamily members, but it lacks an α-helix in the region between the βD and βE strands (17-20).

TIR domains are crucial for TLR/IL-1R signal transduction as they mediate receptor-receptor, receptor-adaptor and adaptor-adaptor interactions. For this reason, they have been the subject of numerous structural and functional studies aimed at identifying the residues participating to homo and hetero interactions (21-26). In the case of MyD88, it was demonstrated that the BB loop of the TIR domain plays a role in homodimerization (22,27,28). Nevertheless, current understanding of the nature of homotypic oligomerization of the MyD88-TIR domain is still limited. Herein, we have performed an extensive structure-function analysis of the MyD88-TIR domain by mutagenesis. Our studies identify new residues (Glu^{183}, Ser^{244} and Arg^{288}) that are requested to insure efficient self-association of MyD88. Modeling studies revealed that Glu^{183}, Ser^{244} and a portion of the BB loop lay in an interface of dimerization between two contiguous TIR domains. Furthermore, we demonstrated that mutation of these residues also impairs the recruitment of IRAK1/4 and the activation of NF-κB. Importantly, forced expression of MyD88 mini-proteins encompassing the Glu^{183} residue competed with homodimerization of the endogenous MyD88 protein and attenuated TLR signalling in immune cells. Thus, our findings identified a novel region of the TIR domain of MyD88 that is crucial for TLR/IL-1R signal transduction.

Experimental procedures

Plasmids—Expression vectors for Flag-tagged MyD88 or Myc-tagged MyD88 TIR, Myc-tagged MyD88, Myc-tagged IRAK1-kinase-dead (KD) (K239S) and Myc-tagged IRAK4-KD (KK213AA), were constructed as previously described (13,27,28). All constructs for the expression of mutated MyD88 TIR or MyD88 were generated by PCR using oligonucleotides containing the mutated residues.

Constructs for GFP-MyD88 fusion proteins expression were obtained by subcloning cDNA encoding each protein into pCL-pCX vector. Lentiviral vectors for stable expression of GFP-MyD88 fusion proteins were constructed by subcloning cDNA encoding each protein into PCCLsin.PPT.hPGK vector. All constructs were confirmed by Cycle Sequencing (BMR Genomics, Padua, Italy). The vector for the expression of Flag-tagged IL-1R was a kind gift from Dr. Alberto Mantovani (Humanitas Clinical and Research Center Rozzano, Italy). The NF-κB-luciferase reporter construct (pNiFty2-Luc) was purchased from InvivoGen, while Renilla luciferase construct (pRL-TK-Luc; Promega).

Cell culture, stimulation and transfections—Human embryonic kidney (HEK) 293T cells were cultured in Dulbecco's modified Eagle's medium, THP-1 cells were maintained in RPMI 1640 medium (Lonza), all supplemented with 10% fetal bovine serum (FBS; Lonza), penicillin and streptomycin (Life Technologies). Dendritic cells were generated from human monocytes of healthy donors. Peripheral blood mononuclear cells (PBMCs) were isolated from buffy coats of healthy blood donor through density gradient centrifugation using Ficoll-Hypaque centrifugation (Amersham Biosciences). Monocytes were then positively separated using anti-CD14-labelled magnetic beads (Miltenyi) and resuspended in RPMI 1640 supplemented with 10% FBS, L-glutamine 2mM, Hepes 10mM, Sodium Piruvate 10mM, non essential amino acids 10mM (Lonza), penicillin and streptomycin (Life Technologies). Monocytes were cultured for 5 days in medium supplemented with 100 ng/mL GM-CSF (Miltenyi) and 40 ng/mL IL-4 (Miltenyi). This protocol leads to 98% to 99% of $CD1a^{+}/CD14^{-}$ monocyte derived dendritic cells (MDDCs). All cells were grown in a 37°C humidified atmosphere of 5% CO2. For Western blot analysis, THP-1 cells were serum-starved overnight in medium containing 0,5% FBS and stimulated or not with Pam3CSK4 (1 μg/ml; InvivoGen) or TNF-α (10 ng/ml; Pepro Tech) for 30 minutes. At the end of incubation, cells were collected, lysed and cell extracts analysed. For flow cytometry analysis the pro-monocytic THP-1 cells were differentiated into mature monocytic cells by treatment with PMA (200 nM) for 24 hours. Mature THP-1 cells and MDDCs were then stimulated with Pam3CSK4 (1 μg/ml; Invivogen) or LPS (1 μg/ml; Sigma Aldhrich), respectively, for 6 h, in presence of Brefeldin A (10 μg/ml) in the last 4 h to inhibit Golgi traffic. At the end of incubation, cells were collected, fixed, permeabilized, stained and analysed by flow cytometry. For co-immunoprecipitation assays, HEK293T cells were cultured in 6-cm-diameter dishes and transfected with the appropriate expression vectors by Lipofectamine 2000 (Life Technologies) according to the manufacturer's instructions. MDDCs were transfected by electroporation with the Amaxa Nucleofector using the Human Dendritic Cell Nucleofector Kit (Lonza) according to the manufacturer's instructions.

Generation of transduced THP-1—THP-1 stable cell lines were generated by transduction with lentiviral vectors encoding GFP or GFP-MyD88 fusion proteins. THP-1 cells ($3x10^5$) were infected with lentiviral particles at a multiplicity of infection (MOI) of 40 in medium supplemented with polybrene (6 μg/ml) for 24h. At the end of incubation, cells were washed in PBS, resuspended in fresh medium and the percentage of GFP-positive cells was assessed by FACS analysis.

Cell extracts and co-immunoprecipitation assay—HEK293T cells were harvested 20 h after transfection, washed in ice-cold PBS, and lysed in buffer containing 50 mM Hepes, pH 7.4, 150 mM NaCl, 1% Nonidet P-40, 20 mM β-glycerophosphate, 2 mM DTT, 1 mM Na_3VO_4, protease inhibitor cocktail (Sigma-Aldrich). After incubating for 10 min on ice, cell lysates were centrifuged at 10,000 x g for 10 min at 4 °C and cytosolic fractions were collected for immunoprecipitation. Cell extracts were immunoprecipitated as described (13,28) using 2 μg of mouse anti-Flag M2 (Sigma-Aldrich) or rabbit anti-GFP antibodies (Molecular Probes). After three washes with lysis buffer, proteins were eluted in SDS sample buffer for Western blot analysis. THP-1 cells were collected 30 min after stimulation, washed in ice-cold PBS, and lysed in buffer containing 50 mM HEPES, pH 7.4, 15 mM MgCl2, 150 mM NaCl, 15 mM EGTA, 10% glycerol, 1% Triton X-100, 20 mM β-glycerophosphate, 1 mM DTT, 1 mM Na_3VO_4, protease inhibitor cocktail (Sigma-Aldrich). Cells were pelleted by centrifugation at 10,000 g for 10 min, and the resulting supernatants were diluted in SDS sample buffer for Western blot analysis.

Western blot analysis—Western-blot analysis were performed as described (13,28) using the following primary antibodies (overnight at 4°C): mouse anti-Myc (1: 1000; Santa Cruz Biotechnology), mouse anti-Flag M2 (1: 3000) and mouse anti-β tubulin (1: 1000; Sigma-Aldrich), rabbit anti-GFP (1: 1000), rabbit anti-phospho-p38 and rabbit anti-phospho-p65 antibodies (1: 1000; Cell Signaling Technology).

NF-κB reporter assay— HEK293T cells ($5x10^5$) were cultured in 24-well plates and transfected with 5 ng of NF-κB-dependent luciferase reporter gene and Renilla luciferase reporter gene (1 ng) as an internal control together with the constructs for the indicated MyD88 proteins by using the Lipofectamine 2000 reagent according to the manufacturer's instructions. THP-1 cells ($1x10^6$) were transfected by electroporation with the Amaxa Nucleofector using the Cell Line Nucleofector® Kit V (Lonza) according to the manufacturer's instructions. Twenty-four hours after transfection, cells were stimulated or not with IL-1β (20 ng/ml), TNF-α (20 ng/ml) or Pam3CSK4 (1 μg/ml) for 6 h. At the end of incubation, cells were harvested, lysed and luciferase activity quantified with a biocounter luminometer using the dual-luciferase reporter assay system (Promega). Data were normalized for transfection efficiency by dividing firefly luciferase activity by that of the Renilla luciferase.

Flow cytometry analysis of cytokine-producing cells— THP-1 cells and MDDCs were stained with live-dead fixable near-infrared (Life Technologies) to exclude dead cells from the subsequent analysis. After washing cells were fixed with 4% paraformaldehyde for 5 min at 4°C, permeabilized in phosphate buffer saline (PBS) supplemented with 0.5% saponin, and stained for 15 min at 4°C with PE-Cy7 conjugated anti-human TNF-α (clone MAb11; eBioscience) or Alexa Fluor 647 anti-human IL-1β (clone JK1B-1; Biolegend). The percentage of cytokine producing cells was analyzed by flow cytometry (Cyan; Beckman Coulter).

Computational analysis – NMR solutions of MyD88 TIR domain (PDB code 2Z5V) were extracted from PDB database (http://www.pdb.org). Models of MyD88-TIR domain homodimer were generated using the algorithm PatchDock and sorted by shape complementarity criteria;

the first twenty solutions were further refined by the FireDock algorithm using a restricted interface side-chain rearrangement and a soft rigid-body optimization. Solutions were automatically ranked by a binding score that includes Atomic Contact Energy, softened van der Waals interactions, partial electrostatics and additional estimations of the binding free energy.

Densitometry and statistical analysis─Densitometric analysis of the Western blots was performed using underexposed images from 3-5 experiments and analysed by the ImageQuant5.0 software. Statistical differences between mean values were determined using the two-tailed Student's t test.

Results

Identification of new residues within the MyD88-TIR domain required for its homodimerization. To identify the residues required for homotypic oligomerization of the TIR domain of MyD88, we performed an extensive mutational analysis. Relying on sequence comparison between different TIR domains (Fig. 1A), we selected several amino acids that might be sensitive to point-mutations. We focused on residues present within the flanking regions of three highly conserved motifs denoted Box 1, 2, and 3 (17) of the MyD88-TIR, with specific attention to charged/polar residues that are likely to be involved in protein-protein interactions (Fig. 1A). We also selected other residues within the AB and CD loops, as they are located in exposed regions that could play a role in the TIR-TIR interface of the MyD88 dimer. The amino acids shown in *boldface type* were substituted with alanine, with the exception of Lys^{282} (isoleucine), Arg^{288} (glycine) and Lys^{291} (methionine) that were substituted with the amino acid requiring the minimal change in codon usage. The effect of the introduced mutation on homodimerization of the TIR domain was then tested by co-immunoprecipitation assays in HEK293T cells co-transfected with Flag-tagged wild-type MyD88 and wild-type or mutated Myc-tagged MyD88-TIR. Cell extracts were immunoprecipitated with anti-Flag antibody and homodimerization was tested by detecting Myc-MyD88-TIR in the immunoprecipitates. We found that several substitutions (D162A, E183A, D195A, K282I and R288G) impaired MyD88-TIR homodimerization with respect to the wild-type TIR domain in this assay (Fig. 1B,C). By contrast, other mutations (N186A, R188A, S242A, S244A, H248A and K291M) were either ineffective or caused a reproducible increase of dimerization (Fig. 1B,C).

Glu^{183}, Ser^{244} and Arg^{288} in the MyD88-TIR domain are required for MyD88 dimerization and IL-1 signaling. Homodimerization of the MyD88-TIR domain is required for propagation of TLR/IL-1R signaling (3,4). Notably, overexpression of MyD88-TIR acts as a dominant-negative inhibitor of signaling, presumably by competing for the interaction between endogenous MyD88 and TLR/IL-1Rs (16,22,24,25). This feature allows the screening for loss-of-function mutations in the TIR domain by testing the recovery of IL-1-dependent activation of NF-κB in transfected cells (22). As expected, overexpression of the wild-type MyD88-TIR domain strongly suppressed IL-1β-dependent expression of an NF-κB reporter gene in transfected cells (Fig. 2A). Screening of the MyD88-TIR mutants by this assay revealed that MyD88-TIR_{E183A}, MyD88-TIR_{S244A} and MyD88-TIR_{R288G} were significantly defective (Fig. 2A), suggesting that Glu^{183}, Ser^{244} and Arg^{288} are key residues in the MyD88-TIR domain.

One surprising aspect of the above results was that although the D162A, E183A, D195A, K282I and R288G mutations similarly reduced homotypic interaction of MyD88-TIR with full length MyD88 (Fig. 1B,C), only MyD88-TIR_{E183A} and MyD88-TIR_{R288G} displayed loss of dominant-negative effect on NF-κB activation (Fig. 2A). Moreover, the MyD88-TIR_{S244A} also lost dominant-negative effect in this assay, despite it strongly interacted with full length MyD88 (Fig. 1B,C). Thus, to further delineate the functional role of these residues in the TIR domain, we introduced the substitution in full length MyD88. We also compared the effect of the novel mutations with that of the L252P substitution (based on the sequence of MyD88 variant 1 used in this study, equivalent to L265P in MyD88 variant 2), which was previously shown to confer oncogenic potential to MyD88 and to constitutively activate downstream signalling (29,30). Overexpression of MyD88 *per se* induces forced protein oligomerization and consequent activation of NF-κB, even in the absence of exogenous stimuli (8). By using an NF-κB-dependent luciferase reporter assay in HEK293T cells, we observed that the $MyD88_{E183A}$, $MyD88_{S244A}$ and $MyD88_{R288G}$ mutants caused 40-60% lower activation of NF-κB than wild-type MyD88, whereas the other mutants activated NF-κB to a similar extent (Fig. 2B). Conversely, $MyD88_{L252P}$ potently activated NF-κB signalling (Fig. 2B). Importantly, expression of $MyD88_{E183A}$, $MyD88_{S244A}$ and $MyD88_{R288G}$ strongly interfered with activation of NF-κB by Pam3CSK4-induced TLR2 signaling pathway in monocytoid THP-1 cells (Fig. 2C). These results suggest that the $MyD88_{E183A}$, $MyD88_{S244A}$ and $MyD88_{R288G}$ mutants exerts a dominant negative effect on endogenous TLR pathways.

In order to assess whether the loss-of-function MyD88 mutants were impaired in their capacity to correctly oligomerize, we carried out co-immunoprecipitation assays. In line with the results of the NF-κB activation assays, we observed that the E183A, S244A and R288G mutations impaired MyD88 homodimerization in HEK293T cells, whereas the other mutants were ineffective and L252P enhanced it (Fig. 2D,E; Table 1).

Homodimerization-defective MyD88 mutants do not recruit IRAKs. After the ligand-induced activation of IL-1R, MyD88 oligomerizes and interacts with the receptor through their respective TIR domains (31). Thus, we investigated whether the Glu^{183}, Ser^{244} and Arg^{288} residues were also required for this heterotypic interaction. HEK293T cells were co-transfected with wild-type or mutated Myc-tagged MyD88 and FLAG-tagged IL-1R. Co-immunoprecipitation experiments indicated that the $MyD88_{E183A}$, $MyD88_{S244A}$ and $MyD88_{R288G}$ mutants are not compromised in their ability to associate with IL-1R (Fig. 3A,B). On the contrary the E183A and R288G mutations even increased interaction between the two proteins.

Oligomerization of MyD88 is required for recruitment of IRAK1/2/4 (12). Thus, we set out to determine the ability of MyD88 loss-of-function mutants to recruit IRAKs. Since the interaction between MyD88 and these kinases is rapid and transient, it can be more reproducibly detected by expressing kinase-dead (KD) derivatives (IRAK1KD and IRAK4KD) (31,32). Wild-type or mutated FLAG-MyD88 were co-expressed with either Myc-tagged IRAK1KD (Fig. 3C) or Myc-tagged-IRAK4KD (Fig. 3E) and cell extracts were immunoprecipitated with anti-FLAG antibodies. MyD88 efficiently associated with IRAK1KD and IRAK4KD, while

$MyD88_{E183A}$, $MyD88_{S244A}$ and $MyD88_{R288G}$ were all impaired in the recruitment of IRAKs (Fig. 3C-F). By contrast, $MyD88_{K282I}$, which is not defective in its ability to oligomerize, interacted with IRAK1/4 like wild-type MyD88 and the constitutively active $MyD88_{L252P}$ was much more efficient that wild-type MyD88 in recruiting IRAKs (Fig. 3C-F). These results suggest that the E183A, S244A and R288G substitutions affect the recruitment of IRAKs by MyD88 as a consequence of their effect on MyD88-TIR dimerization.

Computational modeling of MyD88-TIR homodimer suggests the residues involved in the dimerization surface. In order to evaluate the relevance of the identified residues in the dimerization interface, a computational approach was employed. The structure of the MyD88-TIR domain previously determined by solution NMR spectroscopy (16) was used as template for protein-protein interaction procedures (PDB code; 2Z5V). We then employed the PatchDock algorithm (33,34), which divides protein surfaces into patches according to the surface shape. Finally, the remaining dimers were ranked according to a geometric shape complementarity score. Twenty solutions from PatchDock were further refined using the FireDock algorithm (35,36). Each dimer was refined by restricted interface side-chain rearrangement and by soft rigid-body optimization. Following rearrangement of the side-chains, the relative position of the docking partners was refined by Monte Carlo minimization of the binding score function. This score includes Atomic Contact Energy, softened van der Waals interactions, partial electrostatics and additional estimations of the binding free energy. The refined homodimers were ranked by the binding score (Supplementary Table S1). Analysis of the 20 top-scored solutions showed that only the first one contains Glu^{183} and Ser^{244} in the dimerization interface. Importantly, this solution scored as the most stable one, providing an independent confirmation of the relevance of Glu^{183} and Ser^{244} for MyD88-TIR homodimerization. These studies yielded an hypothetical model for MyD88-TIR homodimerization wherein Glu^{183} in the first monomer (blue) interacts with the αC' helix in the second monomer (yellow) (Fig. 4). Moreover, Ser^{244} in the second monomer interacts with the N-terminal fragment (aa 156-158) in the first monomer that is structured and exposed to the solvent.

GFP-MyD88 mini-proteins encompassing the Glu^{183} region specifically interfere with IL-1-dependent NF-κB activation. The Glu^{183} residue is located at the junction between the αA helix and the loop that connects it to the BB loop of the TIR domain (Fig. 4), which was previously reported to influence MyD88 homodimerization and signalling (22,27). Given the relevance of this region of the TIR domain for MyD88 function, we investigated it in further detail. First, to determine whether the expression of regions of MyD88-TIR encompassing the Glu^{183} residue can compete with the scaffold function of MyD88 and affect IL1-R signal transduction, we generated two green fluorescent protein (GFP)-tagged MyD88 fusion proteins containing different portions of this region: GFP-$MyD88_{151-189}$ and GFP-$MyD88_{168-189}$ (Fig. 5A). Using a reporter gene assay in HEK293T cells, we found that expression of the GFP-MyD88 $MyD88_{151-189}$ and GFP-$MyD88_{168-189}$ fusion proteins significantly reduced the IL-1R-dependent activation of NF-κB (by ~30%, Fig. 5B). Importantly, the effect of these mini-proteins was specific, since they did not inhibit activation of NF-κB by the MyD88-independent TNF-α pathway (Fig. 5B).

To investigate whether the inhibitory effect of the GFP-MyD88 mini-proteins on IL-1β signaling was due to their ability to titrate out endogenous MyD88, first we tested whether they were able to interact with the MyD88-TIR domain by co-immunoprecipitation assays. GFP, GFP-MyD88, GFP- $MyD88_{151-189}$ and GFP- $MyD88_{168-189}$ were co-expressed in HEK293T cells with Myc-tagged MyD88-TIR. As expected, GFP-MyD88 interacted with MyD88-TIR (Fig. 5C). GFP- $MyD88_{151-189}$ and GFP- $MyD88_{168-189}$ also associated with the TIR domain, albeit with less efficiency (Fig. 5C). Despite the weaker interaction with MyD88-TIR, this experiment suggests that these GFP-MyD88 mini-proteins are folded correctly and maintain the original structure. Next, we investigated whether they were able to inhibit the activation of NF-κB by virtue of their interference with MyD88-TIR homodimerization. HEK293T cells were co-transfected with Myc-MyD88-TIR alone or in combination with FLAG-MyD88 in the presence of GFP, GFP- $MyD88_{151-189}$ and GFP- $MyD88_{168-189}$. Co-immunoprecipitation experiments showed that expression of the two MyD88 miniproteins reduced MyD88-TIR homodimerization (Fig. 5D), whereas expression of GFP protein alone exerted no effect. Hence, these results indicate that the GFP-MyD88 mini-proteins impair IL-1R signaling by interfering with homodimerization of its TIR domain.

A MyD88 mini-protein encompassing the Glu^{183} region interferes with TLR signaling in monocytoid cells. Hyperactivation of the TLR/IL-1R signal transduction pathway is involved in several autoinflammatory and autoimmune diseases (1,2). Thus, agents that limit the activation of this pathway are of potential therapeutic interest. Given the dominant negative effect of the GFP-MyD88 mini-proteins on the IL-1β-signaling pathway, we asked whether they can also affect activation of TLR signaling in cells of relevance for immune system disorders. To test this possibility, we analyzed their effect on activation/phosphorylation of the endogenous p38 (14) and p65, a subunit of NF-κB (37), after stimulation of TLR2 in monocytoid cells (38). THP-1 cells were transduced by lentiviral particles to express GFP- $MyD88_{151-189}$, or GFP-$MyD88_{168-189}$, or GFP as control. Transduction efficiency (100%) was evaluated by flow cytometry analysis (Fig. 6A). Flow cytometry (Fig. 6A) and Western blot analysis (Fig. 6B,E) of the transduced THP-1 cells showed that GFP was expressed at high levels, GFP-$MyD88_{151-189}$ was expressed at low levels, whereas the expression of GFP-$MyD88_{168-189}$ was detected at intermediate levels. Importantly, in THP-1 stimulated with the TLR2 ligand Pam3CSK4, expression of the two MyD88 miniproteins caused a significant reduction of p38 (Fig. 6B,C) and p65 phosphorylation (Fig. 6B,D). GFP-$MyD88_{168-189}$ was more efficient in inhibiting the TLR2 signaling than GFP-$MyD88_{151-189}$, possibly due to its higher expression levels. Moreover, the inhibitory effect of two MyD88 mini-proteins on TLR2 signaling was specific because they did not interfere with phosphorylation of p38 and p65 induced by TNF-α (Fig. 6E-G), which activates a MyD88-independent signaling pathway (37).

Activation of TLRs in monocytoid cells induces the secretion of cytokines such as TNF-α and IL-1β (1). Thus, we tested the ability of GFP-$MyD88_{168-189}$ to interfere with production of TNF-α and IL-1β in THP1 stimulated with Pam3CSK4. We found that the percentage of cytokine producing cells (within the alive GFP positive cells) was significantly reduced in Pam3CSK4-stimulated THP-1 cells expressing GFP- $MyD88_{168-189}$ (Fig. 7A-C). Even more importantly, we observed that expression of GFP-$MyD88_{168-189}$ reduced the frequency of TNF-α producing

cells in a primary human myeloid cell type, such as the MDDCs. In fact, the percentage of MDDCs that produce TNF-α after LPS stimulation was significantly lower in cells transfected with GFP-MyD88$_{168-189}$ than in control GFP-expressing cells (Fig. 7D,E). These results indicate that a MyD88 mini-protein encompassing the Glu^{183} residues interferes not only with IL-1R signaling but also with TLR pathways in live cells.

Discussion

MyD88 is an adaptor protein that plays a pivotal role in immune responses mediated by TLR/IL-1Rs. Upon ligand binding, these receptors homo- or heterodimerize through their TIR domains and recruit MyD88, which in turn dimerizes via its DD or TIR domain to nucleate a macromolecular complex named Myddosome (12,39). The TIR domain is a cytoplasmic domain typically composed of 135-160 residues, with sequence conservation between 20 and 30% in different proteins. The sequence and structure of different TIR domains determine the specificities of receptor and adaptor protein TIR-TIR interactions. A number of mutagenesis and docking studies have identified different TIR-TIR interfaces of interaction (16-27). The BB loop, which forms a protrusion on the surface of the TIR domain (17), has been particularly studied (16,17,22,27,28, 40,41,42,43). In the case of MyD88-TIR, the BB loop is involved in both adaptor-receptor and adaptor-adaptor interactions, as documented by its role in the association between MyD88 and TLR4 (16), IL-1RacP (22) and TLR2 (24) as well as in MyD88 homodimerization (22,27,28). Nevertheless, given the plasticity and heterogeneity of complexes formed by this domain in MyD88, it is likely that additional regions of the TIR also play a key role in the interaction with TLR/IL1-R receptors and/or in the assembly of the Myddosome.

The identification of amino acidic stretches potentially involved in TIR-TIR interactions can be exploited to develop specific inhibitors of TLR/IL-1R signal transduction pathways. Such compounds would represent a valuable therapeutic tool to counteract the aberrant stimulation of these pathways that occur in a multitude of human diseases, such as cancer, autoimmune, chronic inflammatory or infectious diseases (44-48). We and others have previously shown that short amino acidic stretches can serve as templates to design decoy peptides and synthetic analogues (peptidomimetics) that interfere with TIR-TIR interactions and down-regulate TLR/IL-1R signaling (44-46). Regarding MyD88, a synthetic peptide encompassing the conserved residues of the BB loop was shown to compromise MyD88 self-association and to interfere with IL-1R-dependent signal transduction (27). Moreover, we developed a synthetic compound (ST2825) mimicking the BB loop peptide and demonstrated that it was efficient in inhibiting IL-1R and TLR9 signaling pathways (28,49). Notably, since MyD88 plays a crucial role in the activation of the signaling pathways triggered by all TLR/IL-1Rs, with the sole exception of TLR3 (9), it represents a suitable target for diseases in which aberrant regulation of TLR/IL-1R signalling contributes to the pathology (44,45). In this study, we have performed an extensive mutational analysis of the MyD88-TIR domain to identify new regions involved in MyD88 homodimerization. We identified several residues that affect the interaction of the isolated MyD88-TIR with full length MyD88. Individual mutation of Asp^{162} (box1), Glu^{183} (αA helix/AB loop), Asp^{195} (BB loop), Lys^{282} and Arg^{288} (flanking regions box 3) inhibited MyD88-TIR homodimerization in co-immunoprecipitation experiments. Notably, mutation of other residues, such as Asn^{186} (AB loop), Arg^{188} (AB loop), Ser^{242} (CD loop), Ser^{244} (CD loop), His^{248} (CD loop) and Lys^{291} (flanking region box 3), caused an increased association of the TIR domain with full length MyD88 in the same assay. However, even if all these residues affected in some way the homotypic interaction of the TIR domain, only the Glu^{183}, Ser^{244} and Arg^{288} were required for IL-1R and TLR signal transduction in live cells. These results suggest that decreased or increased homodimerization in transfection experiments is not sufficient to explain the activity of MyD88. It is possible that the MyD88-TIR mutants that are still capable to support IL-1R/TLR signal transduction undergo conformational changes in the cell that make them behave like the wild-type MyD88-TIR, even though their homodimerization efficiency is altered. It is also worth notice that these types of experiments are generally performed under overexpression conditions, which may represent a less sensitive system to detect mild defects in protein functions. Nevertheless, these studies allowed us to identify Glu^{183}, Ser^{244} and Arg^{288} as residues that are strictly required for the function of full length MyD88. First, these amino acids were necessary for efficient homodimerization of the full length protein, even though MyD88 mainly homodimerizes through the DD and ID (16). Moreover, mutation of these residues interfered with the ability of MyD88 to activate NF-κB in response to IL-1β and Pam3CSK4 stimulation, indicating that their effect on homodimerization was functionally relevant. Surprisingly, the S244A mutation induced an increase in homodimerization of the isolated MyD88-TIR, whereas it reduced self-association of the full length protein, suggesting that in the context of full length MyD88 the presence of the DD and ID might induce conformational rearrangements of the MyD88 dimer that affect the homotypic oligomerization of TIR domains and the specific contacts engaged by the exposed residues.

To fit our results in a three-dimensional model, we employed a computational approach based on the documented NMR structure of the TIR domain of MyD88. The resulting model provides some hints on how these three aminoacids could stabilize TIR domain homodimerization. Indeed, in the lowest energy model Glu^{183} and Ser^{244} are directly involved in the dimerization interface. This model also predicts that residues Phe^{235} and Lys^{238}, located in the αC' helix, are involved in the interaction with αA helix containing Glu^{183}. Moreover, aminoacids at the N-terminal of the monomer are faced towards Ser^{244}. On the contrary, Arg^{288} is far away from this interface but lays within a very long and structured loop that could be stabilized by a salt bridge interaction between Arg^{288} and Asp^{275} or, alternatively, between Asp^{275} and Lys^{256}, thus enhancing loop plasticity in respect to possible heterodimeric interactions. Noteworthy, our study identifies new functional surface sites in the MyD88-TIR that are important for homodimerization. The Glu^{183} and Ser^{244} residues are located at the end of the αA helix and in the CD loop, respectively. To our knowledge, this is the first evidence of an involvement of these portions in the homodimerization of MyD88-TIR. The Arg^{288} residue flanks the highly conserved box 3 and was reported to participate in TIR-TIR interactions between MyD88 and MAL (16), TLR2 (24) and TRAM (25). Herein, we extend these findings by showing that Arg^{288} residue is also involved in MyD88 homodimerization, suggesting that this extended loop plays a general role in TIR:TIR homo- and hetero-dimerization. Our model of the MyD88 TIR:TIR homodimer was generated using the experimental data reported in this work. Future studies by site-directed

mutagenesis (for instance of Lys^{238} and Asp^{275}) and the synthesis of small peptides derived by αA and αC′ helixes could be suitable approaches to identify the smallest active portion interfering with MyD88 signalling in live cells.

In our model, Glu^{183} is located in an accessible interface between the two MyD88-TIR monomers. To test this hypothesis, we engineered small MyD88 mini-proteins encompassing Glu^{183} ($MyD88_{151-189}$ and $MyD88_{168-189}$) and expressed them as fusions with GFP in eukaryotic cells. These mini-proteins were capable of interfering with MyD88 self-association, indicating that the N-terminal region of the MyD88-TIR domain, comprising the βA β-sheet, AA loop, αA helix and AB loop (151–189 residues), is required for homotypic oligomerization. Moreover, the efficient competition exerted by these mini-proteins suggests that this interface region between two TIR domains is under a dynamic and exchangeable equilibrium, which is accessible to competing molecules. In support of this notion, we also found that these mini-proteins hampered IL-1β-induced activation of NF-κB in transfected cells, indicating that their inhibitory effect on MyD88 dimerization is functionally relevant. Furthermore, retroviral infection of these GFP-MyD88 mini-proteins in the human THP-1 monocytic cell line decreased the activation TLR2 signaling and down-regulated the production of TNF-α and IL-1β after stimulation of cells with Pam3CSK4. This observation is of considerable importance as TNF-α and IL-1β are pro-inflammatory cytokines involved in many autoinflammatory and autoimmune diseases and modulation of their secretion from innate immune cells might represent a suitable target for therapeutic intervention (44-47). In this regard, we also tested the ability of the MyD88 mini-proteins to modulate TLR responses in primary immune cells of relevance for human diseases, such as monocyte-derived dendritic cells. Dendritic cells express a broad repertoire of TLRs through which they recognize different microbial compounds (50). After challenge with microbial stimuli, they undergo a complex process of maturation, including cytokine production, that results in the activation of an appropriate adaptive immune response (51). We found that the GFP-$MyD88_{168-189}$ mini-protein is able to decrease the percentage of dendritic cells that produce TNF-α upon TLR2/TLR4 stimulation. Since dendritic cells play a key role in immune regulation, the observation that the GFP-$MyD88_{168-189}$ mini-protein interferes with their TLR-induced response is potentially relevant for several diseases caused by excessive inflammatory responses, such as chronic diseases (i.e. atherosclerosis, Alzheimer's disease) or autoimmune diseases (i.e. multiple sclerosis, Chron's diseases, psoriasis) (52). On the other hand, the identification of critical residues for the MyD88 function in dendritic cells might be of relevance for genetic diseases associated with microbial susceptibility. In this regard, our previous mutational study of the DD of MyD88 identified a crucial residue (Glu^{52}) (13) that was found mutated in children affected by life-threatening recurrent pyogenic bacterial infections (53).

In conclusion, we provide evidence that Glu^{183}, Ser^{244} and Arg^{288} are involved in the homotypic oligomerization of the TIR domain of MyD88. Our study also reveals that a short region in this domain encompassing Glu^{183} forms a critical surface in the interaction between two TIR domains. These results suggest that this amino acidic stretch could serve as template to design peptides and peptidomimetics that might behave as decoy molecules and compete with the endogenous MyD88, thus interfering with the activation of an aberrant TLR/IL-1R signal transduction in various pathological conditions (44-48).

References

1. Kawai, T., and Akira, S. (2011) Toll-like receptors and their crosstalk with other innate receptors in infection and immunity. Immunity 34, 637-650
2. Sims, J. E., and Smith, D. E. (2010) The IL-1 family: regulators of immunity. Nat. Rev. Immunol. 10, 89-102
3. O'Neill, L. A. (2008) The interleukin-1 receptor/Toll-like receptor superfamily: 10 years of progress. Immunol. Rev. 226,10-18.
4. O'Neill, L. A., and Bowie, A. G. (2007) The family of five: TIR domain-containing adaptors in Toll-like receptor signalling. Nat. Rev. Immunol. 7, 353-364
5. Roach, J. C., Glusman, G., Rowen, L., Kaur, A., Purcell, M. K., Smith, K. D., Hood, L. E., and Aderem A. (2005) The evolution of vertebrate Toll-like receptors. Proc. Natl. Acad. Sci. USA 102, 9577-9582
6. Sasai, M., and Yamamoto, M. (2013) Pathogen recognition receptors: ligands and signaling pathways by toll-like receptors. Int. Rev. Immunol. 32, 116-133
7. Muzio, M., Ni, J., Feng, P., and Dixit, V. M. (1997) IRAK (Pelle) family member IRAK-2 and MyD88 as proximal mediators of IL-1 signaling. Science 278, 1612-1615
8. Medzhitov, R., Preston-Hurlburt, P., Kopp, E., Stadlen, A., Chen, C., Ghosh, S., and Janeway, C. A. (1998) MyD88 is an adaptor protein in the hToll/IL-1 receptor family signaling pathways. Mol. Cell. 2, 253-258
9. Alexopoulou, L., Holt, A. C., Medzhitov, R., and Flavell, R. A. (2001) Recognition of double-stranded RNA and activation of NF-kappaB by Toll-like receptor 3. Nature 413, 732-738
10. Hardiman, G., Rock, F. L., Balasubramanian, S., Kastelein, R. A., and Bazan, J. F. (1996) Molecular characterization and modular analysis of human MyD88. Oncogene 13, 2467-2475
11. Park, H. H., Lo, Y-C., Lin, S-C., Wang, L., Yang, J. K., and Wu, H. (2007) The death domain superfamily in intracellular signaling of apoptosis and inflammation. Annu. Rev. Immunol. 25, 561-586
12. Lin, S. C., Lo, Y. C., and Wu, H. (2010) Helical assembly in the MyD88-IRAK4-IRAK2 complex in TLR/IL-1R signaling. Nature 465, 885-890
13. Loiarro, M., Gallo, G., Fantò, N., De Santis, R., Carminati, P., Ruggiero, V., and Sette, C. (2009) Identification of critical residues of the MyD88 death domain involved in the recruitment of downstream kinases. J. Biol. Chem. 284, 28093-28103
14. Brown, J., Wang, H., Hajishengallis, G. N., and Martin, M. (2011) TLR-signaling networks: an integration of adaptor molecules, kinases, and cross-talk. J. Dent. Res. 90, 417-427
15. Burns, K., Janssens, S., Brissoni, B., Olivos, N., Beyaert, R., and Tschopp, J. (2003) Inhibition of interleukin 1 receptor/Toll-like receptor signaling through the alternatively spliced, short form of MyD88 is due to its failure to recruit IRAK-4. J. Exp. Med. 197, 263-268
16. Ohnishi, H., Tochio, H., Kato, Z., Orii, K. E., Li, A., Kimura, T., Hiroaki, H., Kondo, N., and Shirakawa, M. (2009) Structural basis for the multiple interactions of the MyD88 TIR domain in TLR4 signaling. Proc. Natl. Acad. Sci. U S A. 106, 10260-10265
17. Xu, Y., Tao, X., Shen, B., Horng, T., Medzhitov, R., Manley, J. L., and Tong, L. (2000) Structural basis for signal transduction by the Toll/interleukin-1 receptor domains. Nature 408, 111-115
18. Nyman, T., Stenmark, P., Flodin, S., Johansson, I., Hammarström, M., and Nordlund, P. (2008) The crystal structure of the human Toll-like receptor 10 cytoplasmic domain reveals a putative signaling. J. Biol. Chem. 283,11861-11865
19. Khan, J. A., Brint, E. K., O'Neill, L. A., and Tong, L. (2004) Crystal structure of the Toll/interleukin-1 receptor domain of human IL-1RAPL. J. Biol. Chem. 279, 31664-31670
20. Valkov, E., Stamp, A., Dimaio, F., Baker, D., Verstak, B., Roversi, P., Kellie, S., Sweet, M. J., Mansell, A., Gay, N. J., Martin, J. L., and Kobe, B. (2011) Crystal structure of Toll-like receptor adaptor MAL/TIRAP reveals the molecular basis for signal transduction and disease protection. Proc. Natl. Acad. Sci. U S A 108, 14879-14884
21. Radons, J., Dove, S., Neumann, D., Altmann, R., Botzki, A., Martin, M. U., and Falk, W. (2003) The interleukin 1 (IL-1) receptor accessory protein Toll/IL-1 receptor domain: analysis of putative interaction sites in vitro mutagenesis and molecular modeling. J. Biol. Chem. 278, 49145-49153
22. Li, C., Zienkiewicz, J., and Hawiger, J. (2005) Interactive Sites in the MyD88 Toll/Interleukin (IL) 1 Receptor Domain Responsible for Coupling to the IL1 Signaling Pathway. J. Biol. Chem. 280, 26152-26159
23. Bovijn, C., Ulrichts, P., De Smet, A. S., Catteeuw, D., Beyaert, R., Tavernier, J., and Peelman, F. (2012) Identification of interaction sites for dimerization and adapter recruitment in Toll/interleukin-1 receptor (TIR) domain of Toll-like receptor 4. J. Biol. Chem. 287, 4088-4098
24. Nada, M., Ohnishi, H., Tochio, H., Kato, Z., Kimura, T., Kubota, K., Yamamoto, T., Kamatari, Y. O., Tsutsumi, N., Shirakawa, M., and Kondo, N. (2012) Molecular analysis of the binding mode of Toll/interleukin-1 receptor (TIR) domain proteins during TLR2 signaling. Mol. Immunol. 52,108-116
25. Ohnishi, H., Tochio, H., Kato, Z., Kawamoto, N., Kimura, T., Kubota, K., Yamamoto, T., Funasaka, T., Nakano, H., Wong, R.W., Shirakawa, M., and Kondo, N. (2012) TRAM is involved in IL-18 signaling and functions as a sorting adaptor for MyD88. PLoS One 7, e38423
26. Bovijn, C., Desmet, A. S., Uyttendaele, I., Van Acker, T., Tavernier, J., and Peelman, F. (2013) Identification of binding sites for Myeloid differentiation primary response gene 88 (MyD88) and Toll-like receptor 4 in MyD88 adapter like (Mal). J. Biol. Chem. 288, 12054-12066
27. Loiarro, M., Sette, C., Gallo, G., Ciacci, A., Fantò, N., Mastroianni, D., Carminati, P., and Ruggiero, V. Peptide-mediated interference of TIR domain dimerization in MyD88 inhibits interleukin-1-dependent activation of NF-{kappa}B. J. Biol. Chem. 280, 15809-15814
28. Loiarro, M., Capolunghi, F., Fantò, N., Gallo, G., Campo, S., Arseni, B., Carsetti, R., Carminati, P., De Santis, R., Ruggiero, V., and Sette, C. (2007) Pivotal Advance: Inhibition of MyD88 dimerization and recruitment of IRAK1 and IRAK4 by a novel peptidomimetic compound. J. Leukoc. Biol. 82, 801-810

29 Ngo, V.N., Young, R.M., Schmitz, R., Jhavar. S., Xiao, W., Lim, K.H., Kohlhammer, H., Xu, W., Yang, Y., Zhao, H., Shaffer, A.L., Romesser, P., Wright, G., Powell, J., Rosenwald, A., Muller-Hermelink, H.K., Ott, G., Gascoyne, R.D., Connors, J.M., Rimsza, L.M., Campo, E., Jaffe, E.S., Delabie, J., Smeland, E.B., Fisher, R.I., Braziel, R.M., Tubbs, R.R., Cook, J.R., Weisenburger, D.D., Chan, W.C., and Staudt, L.M. (2011) Oncogenically active MYD88 mutations in human lymphoma. Nature 470, 115-119
30. Treon, S.P., Xu, L., Yang, G., Zhou, Y., Liu, X., Cao, Y., Sheehy, P., Manning, R.J., Patterson, C.J., Tripsas, C., Arcaini, L., Pinkus, G.S., Rodig, S.J., Sohani, A.R., Harris, N.L., Laramie, J.M., Skifter, D.A., Lincoln, S.E., and Hunter, Z.R. (2012) MYD88 L265P somatic mutation in Waldenstrom's macroglobulinemia. N. Engl. J. Med. 367, 826-833
31. Wesche, H., Henzel, W. J., Shillinglaw, W., Li, S., and Cao, Z. (1997) MyD88: an adapter that recruits IRAK to the IL-1 receptor complex. Immunity 7, 837-847
32. Li, S., Strelow, A., Fontana, E. J., and Wesche, H. (2002) IRAK-4: a novel member of the IRAK family with the properties of an IRAK-kinase. Proc. Natl. Acad. Sci. U.S.A. 99, 5567-5572
33. Duhovny, D., Nussinov, R., and Wolfson, H. J. (2002) Efficient Unbound Docking of Rigid Molecules. In Gusfield et al., Ed. Proceedings of the 2'nd Workshop on Algorithms in Bioinformatics(WABI) Rome, Italy, Lecture Notes in Computer Science 2452, 185-200, Springer Verlag
34. Schneidman-Duhovny, D., Inbar, Y., Nussinov, R., and Wolfson, H. J (2005). PatchDock and SymmDock: servers for rigid and symmetric docking. Nucleic Acids Res. 33, 363-367
35. Andrusier, N., Nussinov, R., and Wolfson, H. J. (2007) FireDock: Fast Interaction Refinement in Molecular Docking. Proteins 69, 139-159
36. Mashiach, E., Schneidman-Duhovny, D., Andrusier, N., Nussinov, R., and Wolfson, H. J. (2008) FireDock: a web server for fast interaction refinement in molecular docking. Nucleic Acids Res. 36, W229-232
37. Napetschnig, J., and Wu, H. (2013) Molecular Basis of NF-κB Signaling. Annu. Rev. Biophys. 42, 443-468
38. Remer, K. A., Brcic, M., Sauter, K. S., and Jungi, T. W. (2006) Human monocytoid cells as a model to study Toll-like receptor-mediated activation. J. Immunol. Methods 313, 1-10.
39. Burns, K., Martinon, F., Esslinger, C., Pahl, H., Schneider, P., Bodmer, J. L., Di Marco, F., French, L., and Tschopp, J. (1998) MyD88, an adapter protein involved in interleukin-1 signaling. J. Biol. Chem. 273, 12203-12209
40. Bartfai, T. Behrens, M. M., Gaidarova, S., Pemberton, J., Shivanyuk, A., and Rebek, J. Jr. (2003) A low molecular weight mimic of the Toll/IL-1 receptor/resistance domain inhibits IL-1 receptor-mediated responses. Proc. Natl Acad. Sci. USA 100, 7971-7976
41. Poltorak, A., He, X., Smirnova, I., Liu, M. Y., Van Huffel, C., Du, X., Birdwell, D., Alejos, E., Silva, M., Galanos, C., Freudenberg, M., Ricciardi-Castagnoli, P., Layton, B., and Beutler, B. (1998) Defective LPS signaling in C3H/HeJ and C57BL/10ScCr mice: mutations in Tlr4 gene. Science 282, 2085-2088
42. Horng, T., Barton, G. M., and Medzhitov, R. (2001) TIRAP: an adapter molecule in the Toll signaling pathway. Nat. Immunol. 2, 835-841
43. Fitzgerald, K. A., Rowe, D. C., Barnes, B. J., Caffrey, D. R., Visintin, A., Latz, E., Monks, B., Pitha, P. M., and Golenbock, D. T. (2003) LPS-TLR4 signaling to IRF-3/7 and NF-kappaB involves the toll adapters TRAM and TRIF. J. Exp. Med. 198, 1043-1055
44. Loiarro, M., Ruggiero, V., and Sette, C. (2010) Targeting TLR/IL-1R signalling in human diseases. Mediators Inflamm. 2010, 674363
45. Loiarro, M., Ruggiero, V., and Sette, C. (2013) Targeting the Toll-like Receptor/Interleukin 1 Receptor Pathway in Human Diseases: Rational Design of MyD88 Inhibitors. Clin. Lymphoma Myeloma Leuk. 13, 222-226
46. Fekonja, O., Avbelj, M., and Jerala, R. (2012) Suppression of TLR signaling by targeting TIR domain-containing proteins. Curr. Protein Pept. Sci. 13, 776-788
47. Verstak, B., Hertzog, P., and Mansell, A. (2007) Toll-like receptor signalling and the clinical benefits that lie within. Inflamm. Res. 56, 1-10
48. Basith, S., Manavalan, B., Yoo, T. H., Kim, S. G., and Choi, S. (2012) Roles of toll-like receptors in cancer: a double-edged sword for defense and offense. Arch. Pharm. Res 35, 1297-1316
49. Capolunghi, F., Rosado, M. M., Cascioli, S., Girolami, E., Bordasco, S., Vivarelli, M., Ruggiero, B., Cortis, E., Insalaco, A., Fantò, N., Gallo, G., Nucera, E., Loiarro, M., Sette, C., De Santis, R., Carsetti, R., and Ruggiero, V. (2010) Pharmacological inhibition of TLR9 activation blocks autoantibody production in human B cells from SLE patients. Rheumatology (Oxford). 49, 2281-2289
50. Iwasaki, A, and Medzhitov, R. (2004) Toll-like receptor control of the adaptive immune responses. Nat. Immunol. 5, 987-995
51. Banchereau, J., and Steinman, R. M. (1998) Dendritic cells and the control of immunity. Nature 392, 245-252
52. Tabas, I, and Glass, C. K. (2013) Anti-inflammatory therapy in chronic disease: challenges and opportunities. Science 339, 166-172
53. von Bernuth, H., Picard, C., Jin, Z., Pankla, R., Xiao, H., Ku, C.L., Chrabieh, M., Mustapha, I. B., Ghandil, P., Camcioglu, Y., Vasconcelos, J., Sirvent, N., Guedes, M., Vitor, A. B., Herrero-Mata, M. J., Aróstegui, J. I., Rodrigo, C., Alsina, L., Ruiz-Ortiz, E., Juan, M., Fortuny, C., Yagüe, J., Antón, J., Pascal, M., Chang, H. H., Janniere, L., Rose, Y., Garty, B. Z., Chapel, H., Issekutz, A., Maródi, L., Rodriguez-Gallego, C., Banchereau, J., Abel, L., Li, X., Chaussabel, D., Puel, A., and Casanova, J. L. (2008) Pyogenic bacterial infections in humans with MyD88 deficiency. Science 321, 691-696

Acknowledgements: We acknowledge Dr. Alberto Mantovani and Dr. Gennaro Melino for generous gift of plasmids and reagents. This work was supported by grants from FISM (Fondazione Italiana Sclerosi Multipla), AICR (Association for International Cancer Research) (to C.S.) and Italian Ministry of Health (Progetto Giovani Ricercatori) (to E.V.)

Figure legends

Fig. 1. Mutation of select residues in MyD88 affect homodimerization of the TIR domain. (A) Sequence alignment of TIR domains of human MyD88, IL-1R, TLR1, TLR2 and TLR4 as the basis of homology modeling performed with ClustalW. Gray bars indicate secondary structure of the MyD88 TIR domain determined by solution NMR spectroscopy (16). White bars indicate the Box 1, 2, and 3, three highly conserved motifs within the TIR domains (17). The asterisks denote identical residues, while the double-dots and single-dot denote conservative or semi conservative substitutions, respectively. In *boldface type* are shown the residues mutated for structure-function studies. (B) Western blot analysis of the effect of site-specific mutations on homodimerization of MyD88-TIR domain. HEK293T cells were transfected with empty vector (lane 1) or Flag-MyD88 (other lanes) in combination with Myc-MyD88-TIR wild-type (WT) or mutated, as indicated. Cell extracts were immunoprecipitated (IP) with anti-Flag antibody and the immunoprecipitated proteins were then analyzed by with either anti-Flag- or anti-Myc-specific antibodies to detect the interaction. (C) Densitometric analysis of the effect of MyD88-TIR mutants on homodimerization of TIR domain. Data are expressed as a percentage of the wild-type ± standard deviation (S.D.) from three separate experiments.

Fig. 2. Functional analysis of MyD88 mutants. (A) HEK293T cells were transfected with NF-κB reporter construct expressing firefly luciferase alone or in combination with wild-type or mutated Myc-MyD88-TIR. Twenty-four hours after transfection, cells were stimulated or not with IL-1β (20 ng/ml) for 6 h and lysed for biocounter luminometer analysis. Data are normalized for transfection efficiency (see Materials and Methods) and each column of graph indicates the relative luciferase activity of the stimulated cells over the non-stimulated cells. Data are expressed as a percentage of inhibition of IL-1β response ± S.D. from three separate experiments. Statistical significance was determined by Student's t test. *, $p<0.05$. Gray bars indicate the mutants that exerted a significant increase of NF-κB activity in comparison with the wild-type protein. (B) HEK293T cells were transiently transfected with wild-type (WT) or mutant MyD88 constructs together with NF-κB-luciferase reporter construct. Data were normalized for transfection efficiency as above and expressed as a percentage of wild type ± S.D. from three separate experiments. Gray bars indicate the defective MyD88 mutants. (C) THP-1 cells were transfected with NF-κB reporter construct expressing firefly luciferase alone or in combination with wild-type or mutated Myc-MyD88. Twenty-four hours after transfection, cells were stimulated or not with Pam3CSK4 (1μg/ml) for 6 h and lysed for biocounter luminometer analysis. Data are normalized for transfection efficiency as described in Materials and Methods and each column of graph represents the relative luciferase activity of the stimulated cells over the non-stimulated cells. Data are expressed as a percentage of inhibition of TLR2 response ± S.D. from three separate experiments. (D) Representative Western blot analysis of the effect of selected mutations on MyD88 homodimerization. HEK293T cells were transfected with Flag-MyD88 in combination with wild-type (lane 1 and 6) or mutated (lanes 2-5 and 7) Myc-MyD88. Cell extracts were immunoprecipitated (IP) with anti-Flag antibody and the immunoprecipitated proteins were then analysed with either anti-Flag or anti-Myc-specific antibodies to detect the interaction. (E) Densitometric analysis of the effect of MyD88 mutants used in (C) on MyD88 homodimerization. Data are expressed as a percentage of the wild type ± S.D. from three separate experiments.

Fig. 3. MyD88 loss-of-function mutants interacts with IL-1R but fail to recruit IRAK1 and IRAK4. (A) Interaction of MyD88 mutants with IL-1R. HEK293T cells were transfected with empty vector (lane 1) or Flag-IL-1R (lanes 2-5) in combination with Myc-MyD88 wild-type (WT) (lane 1-2) or mutated (lanes 3-5). Twenty hours after transfection, cells were collected, and interaction between MyD88 and IL-1R evaluated by co-immunoprecipitation. Cell extracts were immunoprecipitated (IP) with anti-Flag antibody and the immunoprecipitated proteins were then analysed by Western blotting with either anti-Flag- or anti-Myc-specific antibodies to detect the interaction. (B) Densitometric analysis of the effect of MyD88 mutants used in A on its interaction with IL-1R. Data are expressed as a percentage of the wild type ± S.D. from three separate experiments. (C and E) Western blot analysis of the interaction of MyD88 mutants with IRAK1 (C) and IRAK4 (E). HEK293T cells were transfected with empty vector (lane 1, C and E) or wild-type (lane 2, C and E) or mutated (lanes 3-6, C and E) Flag-MyD88 in combination with Myc-IRAK1KD (C) or Myc-IRAK4KD (E). Cell extracts were immunoprecipitated with anti-Flag antibody and the immunoprecipitated proteins analyzed with either anti-Flag- or anti-Myc-specific antibodies to reveal the interaction. (D-F) Densitometric analysis of the interaction between MyD88 and IRAKs used in C and E. Data are expressed as a percentage of the wild type ± S.D. from three separate experiments.

Fig. 4. Model of MyD88-TIR domain homodimerization. Modeling of a MyD88-TIR dimer was perfomed by a computational approach using the available NMR structure as template (16) and the PatchDock and FireDock algorithms. Glu^{183} and Pro^{200} are shown on the first monomer (blue); Ser^{244} and Arg^{288} are shown on the second monomer (yellow).

Fig. 5. GFP-MyD88$_{151-189}$ and GFP-MyD88$_{168-189}$ interfere with IL-1β-induced NF-κB activation. (A) Schematic representation of GFP-MyD88 mini-proteins. (B) NF-κB activity luciferase reporter assay. HEK293T cells were transfected with GFP, GFP-MyD88$_{151-189}$ or GFP-MyD88$_{168-189}$ together with NF-κB luciferase reporter construct and stimulated or not with either 20 ng/ml IL-1β (light gray bars) or 20 ng/ml TNF-α (dark gray bars) for 6 h. Data were normalized for transfection efficiency as described in Fig. 2 and expressed as mean-fold induction±S.D., compared with control expressing GFP from three experiments. Statistical significance was determined by Student's t test. *, $p<0.05$; **, $p<0.01$. (C) GFP-MyD88$_{151-189}$ and GFP-MyD88$_{168-189}$ interact with MyD88-TIR domain. HEK293T cells were transfected with Myc-MyD88-TIR in combination with GFP (lane 1), GFP-MyD88 (lane 2), or GFP-MyD88$_{151-189}$ and GFP-MyD88$_{168-189}$ (lanes 3 and 4, respectively). Cell extracts were immunoprecipitated (IP) with anti-GFP antibody, and immunoprecipitated proteins were

analyzed by Western blot with either anti-GFP- or anti-Myc-specific antibodies. Densitometric analysis of the degree of interaction of Myc-MyD88-TIR with GFP-MyD88, GFP-MyD88$_{151-189}$ or GFP-MyD88$_{168-189}$ is shown in the bar graph. (D) GFP-MyD88$_{151-189}$ and GFP-MyD88$_{168-189}$ interfere with the homodimerization of MyD88-TIR domain. HEK293T cells were transfected with Myc-MyD88-TIR alone (lane 1) or in combination with FLAG-MyD88 (lanes 2-4) in the presence of GFP (lanes 1-2), GFP-MyD88$_{151-189}$ (lane 3) or GFP-MyD88$_{168-189}$ (lane 4). Cell extracts were immunoprecipitated with anti-FLAG antibody, and immunoprecipitated proteins were analysed by Western blot with either anti-FLAG- or anti-Myc-specific antibodies. Densitometric analysis of MyD88-TIR homodimerization in the presence of GFP or GFP-MyD88 fusion proteins is shown and is expressed as percentage of interaction with respect to GFP.

Fig. 6. GFP-MyD88$_{151-189}$ and GFP-MyD88$_{168-189}$ specifically interfere with TLR2 signaling in THP-1 cells. (A) THP-1 cells were transduced with lentiviral particles for stable expression of GFP or GFP-MyD88 mini-proteins (GFP-MyD88$_{151-189}$ and GFP-MyD88$_{168-189}$). The percentage of infected cells was determined by flow cytometry comparing the percentage of GFP fluorescent cells (simple, dotted and dashed lines for GFP control, GFP-MyD88$_{151-189}$ and GFP-MyD88$_{168-189}$ respectively) to uninfected cells (gray solid line). (B,E) Western blot analysis of phospho-p38 (p-p38) and phospo-p65 (p-p65) expression levels in pro-monocytic THP-1 cells. Cells were transduced with lentiviral particles for stable expression of GFP or GFP-MyD88 mini-proteins. After transduction, cells were serum-starved overnight in medium containing 0,5% FBS and stimulated or not with Pam3CSK4 (1μg/ml) (B) or TNF-α (10 ng/ml) (E) for 30 minutes and analysed with anti-phospho-p38 (upper panel, B and E), anti-phospho-p65 (middle panel, B and E), or anti-GFP-specific antibodies (lower panel, B and E). (C,D) Densitometric analysis of TLR2-mediated p38 (C) and p65 (D) phosphorylation. (F,G) Densitometric analysis of TNF-α-mediated p38 (F) and p65 (G) phosphorylation. *, $p<0.05$; **, $p<0.01$.

Fig. 7. GFP-MyD88$_{168-189}$ interferes with the production of TNF-α and IL-1β induced by stimulation of TLR2 and TLR4 in human monocytoid cells. (A) The pro-monocytic THP-1 cells stably expressing GFP or GFP-MyD88$_{168-189}$ were differentiated into mature monocytic cells by PMA treatment for 24 hours and stimulated with Pam3CSK4 (1 μg/ml) for 6 h in presence of Golgi inhibitor Brefeldin A (10 μg/ml). The percentage of TNF-α or IL-1β producing cells within GFP positive cells was quantified by intracellular staining with the specific antibodies and flow cytometry analysis. (B,C) bar graph represents quantitative data from three independent experiments (mean ± standard error mean, SEM). * $P < 0.05$ (Paired t test). (D) MDDCs transfected with constructs for transient expression of GFP or GFP-MyD88$_{168-189}$ were stimulated with LPS (1μg/ml) for 6 h in presence of Golgi inhibitor Brefeldin A (10 μg/ml). At the end of incubation, the cells were harvested, and the percentage of TNF-α producing cells within alive GFP positive cells, was quantified by flow cytometry. Quantification of results as in D for three independent experiments performed with cells from three individual donors is reported in E data are represented as mean ± S.E.M. * $P < 0.05$ (Paired t test).

Table 1

Effect of mutations in MyD88 on protein homodimerization

The interaction of MyD88 mutants with MyD88 wild-type was analysed by co-immunoprecipitation assays. The table reports a summary of the results obtained (yes: MyD88 mutants homodimerize with wild-type protein; no: MyD88 mutants are deficient in homodimerization).

Mutation	**Location**	**Homodimerization of MyD88**
D162A	βA	Yes
E183A	αA	No
N186A	AB Loop	Yes
R188A	AB Loop	Yes
D195A	BB Loop	Yes
S242A	CD Loop	Yes
S244A	CD Loop	No
H248A	CD Loop	Yes
L252P	βD	Yes
K282I	αE	Yes
R288G	αE’	No
K291M	αE’	Yes

A

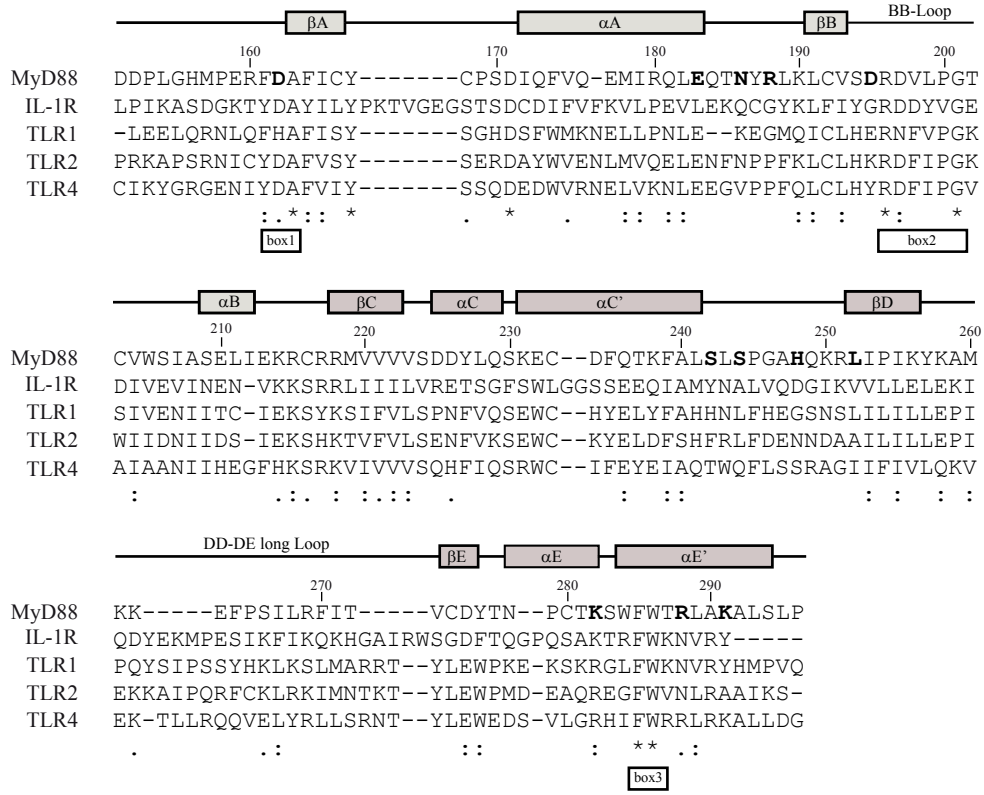
βA
αA
βB
BB-Loop
160
170
180
190
200
MyD88 DDPLGHMPERFDAFICY-------CPSDIQFVQ-EMIRQLEQTNYRLKLCVSDRDVLPGT
IL-1R LPIKASDGKTYDAYILYPKTVGEGSTSDCDIFVFKVLPEVLEKQCGYKLFIYGRDDYVGE
TLR1 -LEELQRNLQFHAFISY-------SGHDSFWMKNELLPNLE--KEGMQICLHERNFVPGK
TLR2 PRKAPSRNICYDAFVSY-------SERDAYWVENLMVQELENFNPPFKLCLHKRDFIPGK
TLR4 CIKYGRGENIYDAFVIY-------SSQDEDWVRNELVKNLEEGVPPFQLCLHYRDFIPGV
box1
box2
αB
βC
αC
αC'
βD
210
220
230
240
250
260
MyD88 CVWSIASELIEKRCRRMVVVVSDDYLQSKEC--DFQTKFALSLSPGAHQKRLIPIKYKAM
IL-1R DIVEVINEN-VKKSRRLIIILVRETSGFSWLGGSSEEQIAMYNALVQDGIKVVLLELEKI
TLR1 SIVENIITC-IEKSYKSIFVLSPNFVQSEWC--HYELYFAHHNLFHEGSNSLILILLEPI
TLR2 WIIDNIIDS-IEKSHKTVFVLSENFVKSEWC--KYELDFSHFRLFDENNDAAILILLEPI
TLR4 AIAANIIHEGFHKSRKVIVVVSQHFIQSRWC--IFEYEIAQTWQFLSSRAGIIFIVLQKV
DD-DE long Loop
βE
αE
αE'
270
280
290
MyD88 KK-----EFPSILRFIT-----VCDYTN--PCTKSWFWTRLAKALSLP
IL-1R QDYEKMPESIKFIKQKHGAIRWSGDFTQGPQSAKTRFWKNVRY-----
TLR1 PQYSIPSSYHKLKSLMARRT--YLEWPKE-KSKRGLFWKNVRYHMPVQ
TLR2 EKKAIPQRFCKLRKIMNTKT--YLEWPMD-EAQREGFWVNLRAAIKS-
TLR4 EK-TLLRQQVELYRLLSRNT--YLEWEDS-VLGRHIFWRRLRKALLDG
box3

B

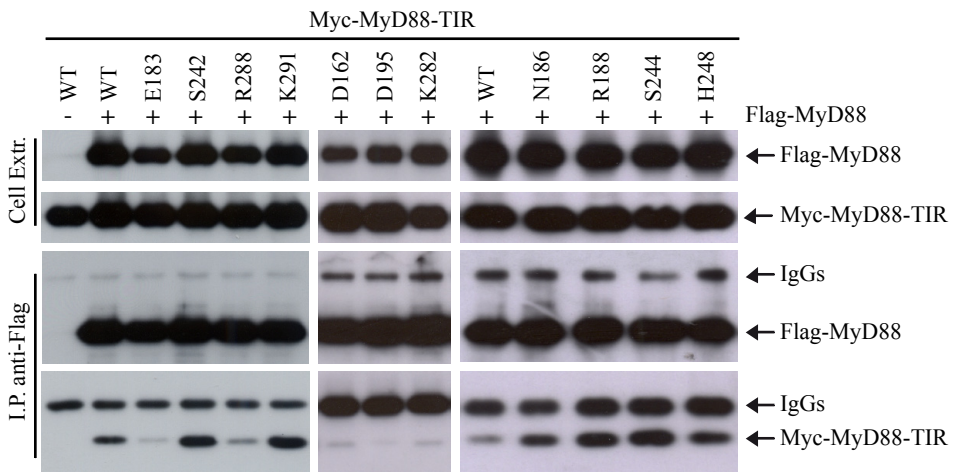
Myc-MyD88-TIR
- WT
+ WT
+ E183
+ S242
+ R288
+ K291
+ D162
+ D195
+ K282
+ WT
+ N186
+ R188
+ S244
+ H248
Flag-MyD88
Cell Extr.
I.P. anti-Flag
Flag-MyD88
Myc-MyD88-TIR
IgGs
Flag-MyD88
IgGs
Myc-MyD88-TIR

C

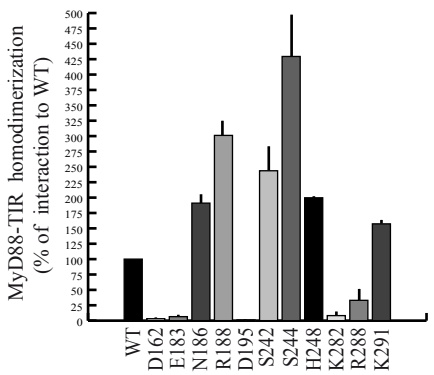
MyD88-TIR homodimerization
(% of interaction to WT)
500
475
450
425
400
375
350
325
300
275
250
225
200
175
150
125
100
75
50
25
0
WT
D162
E183
N186
R188
D195
S242
S244
H248
K282
R288
K291

Figure 1

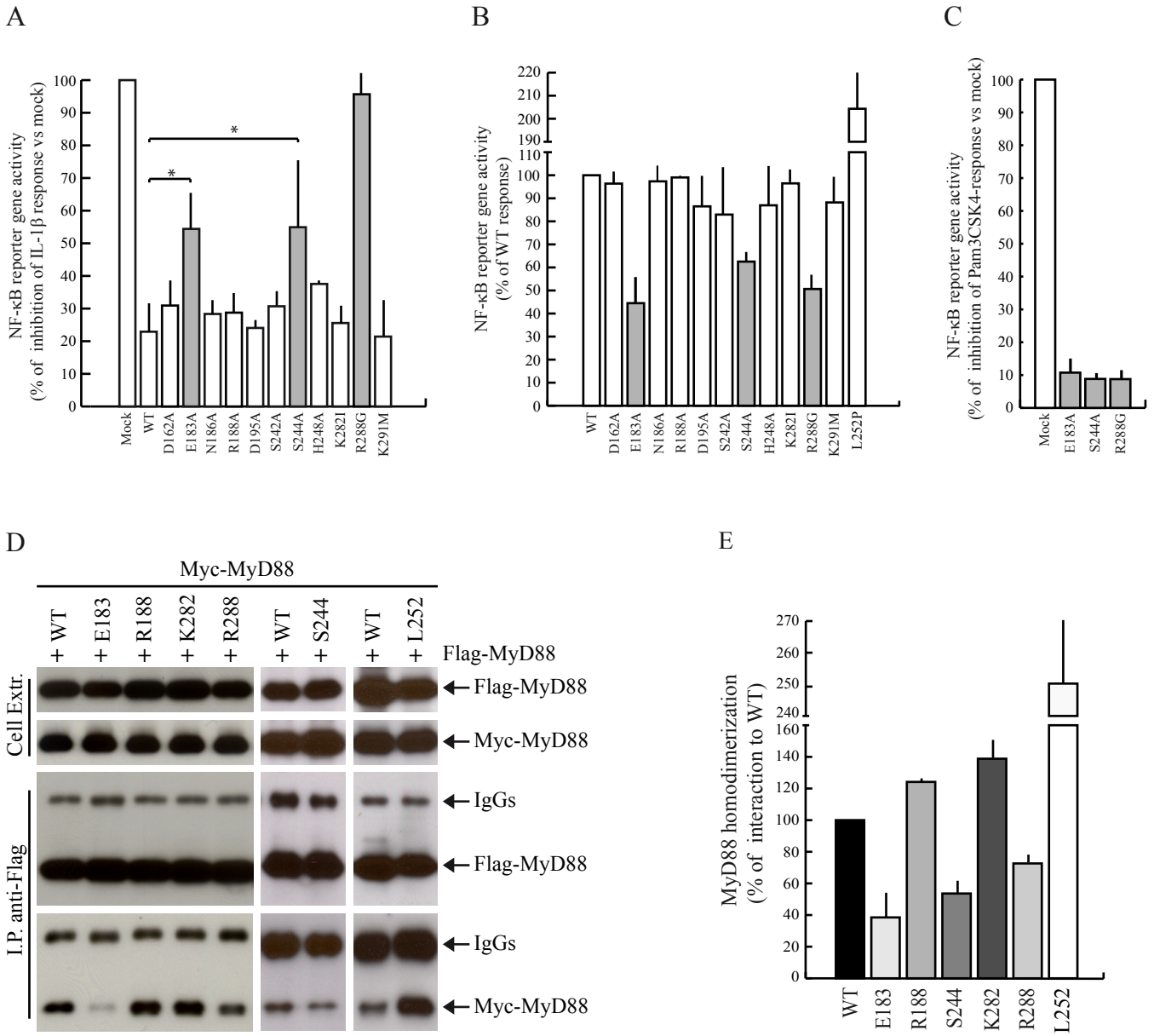
A
NF-κB reporter gene activity
(% of inhibition of IL-1β response vs mock)
Mock
WT
D162A
E183A
N186A
R188A
D195A
S242A
S244A
H248A
K282I
R288G
K291M
B
NF-κB reporter gene activity
(% of WT response)
WT
D162A
E183A
N186A
R188A
D195A
S242A
S244A
H248A
K282I
R288G
K291M
L252P
C
NF-κB reporter gene activity
(% of inhibition of Pam3CSK4-response vs mock)
Mock
E183A
S244A
R288G
D
Myc-MyD88
+ WT
+ E183
+ R188
+ K282
+ R288
+ WT
+ S244
+ WT
+ L252
Flag-MyD88
Cell Extr.
Flag-MyD88
Myc-MyD88
I.P. anti-Flag
IgGs
Flag-MyD88
IgGs
Myc-MyD88
E
MyD88 homodimerization
(% of interaction to WT)
WT
E183
R188
S244
K282
R288
L252

Figure 2

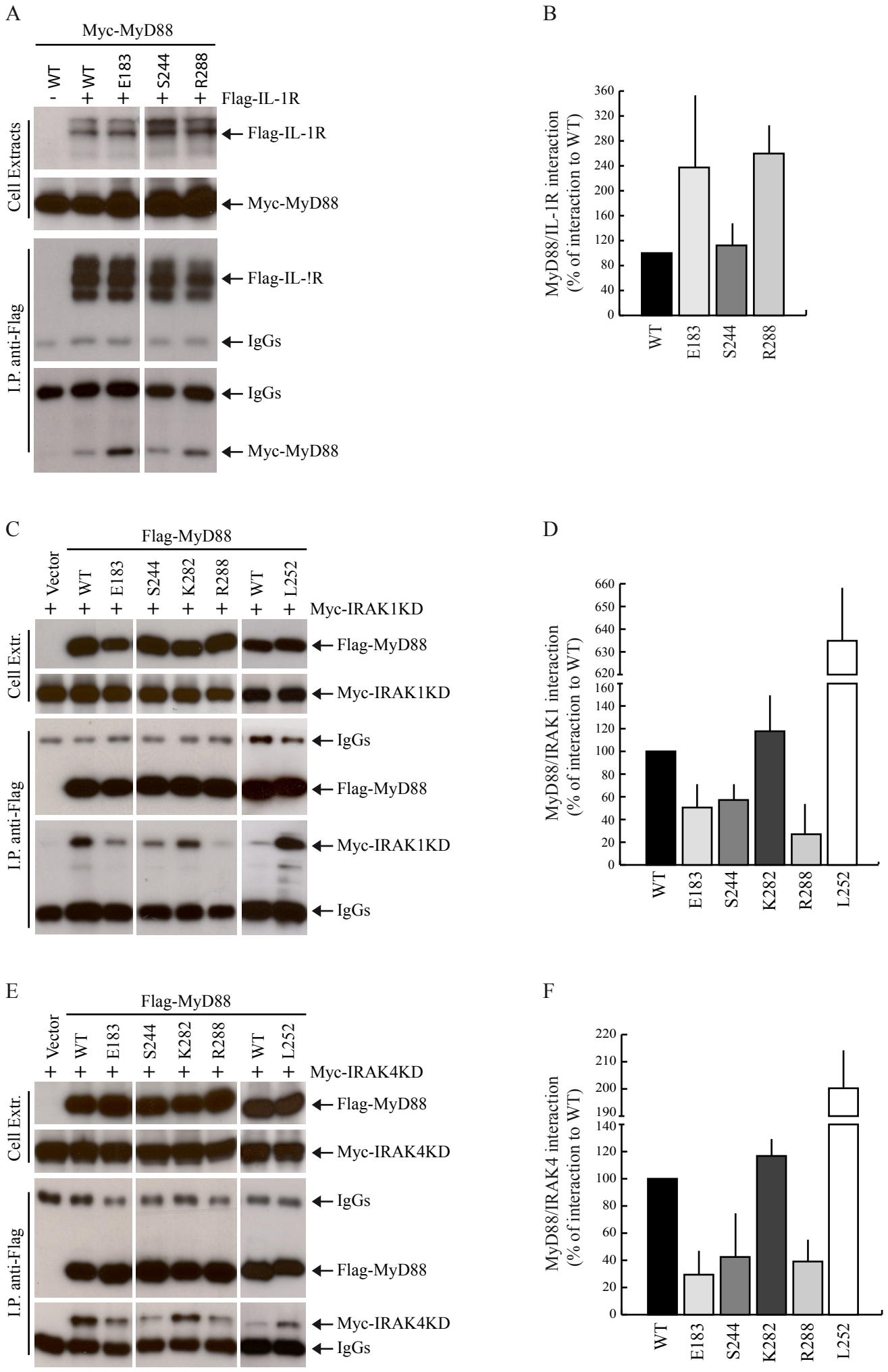
A
Myc-MyD88
- WT
+ WT
+ E183
+ S244
+ R288
Flag-IL-1R
Cell Extracts
← Flag-IL-1R
← Myc-MyD88
I.P. anti-Flag
← Flag-IL-!R
← IgGs
← IgGs
← Myc-MyD88
B
MyD88/IL-1R interaction
(% of interaction to WT)
360
320
280
240
200
160
120
80
40
0
WT
E183
S244
R288
C
Flag-MyD88
+ Vector
+ WT
+ E183
+ S244
+ K282
+ R288
+ WT
+ L252
Myc-IRAK1KD
Cell Extr.
← Flag-MyD88
← Myc-IRAK1KD
I.P. anti-Flag
← IgGs
← Flag-MyD88
← Myc-IRAK1KD
← IgGs
D
MyD88/IRAK1 interaction
(% of interaction to WT)
660
650
640
630
620
160
140
120
100
80
60
40
20
0
WT
E183
S244
K282
R288
L252
E
Flag-MyD88
+ Vector
+ WT
+ E183
+ S244
+ K282
+ R288
+ WT
+ L252
Myc-IRAK4KD
Cell Extr.
← Flag-MyD88
← Myc-IRAK4KD
I.P. anti-Flag
← IgGs
← Flag-MyD88
← Myc-IRAK4KD
← IgGs
F
MyD88/IRAK4 interaction
(% of interaction to WT)
220
210
200
190
140
120
100
80
60
40
20
0
WT
E183
S244
K282
R288
L252

Figure 3

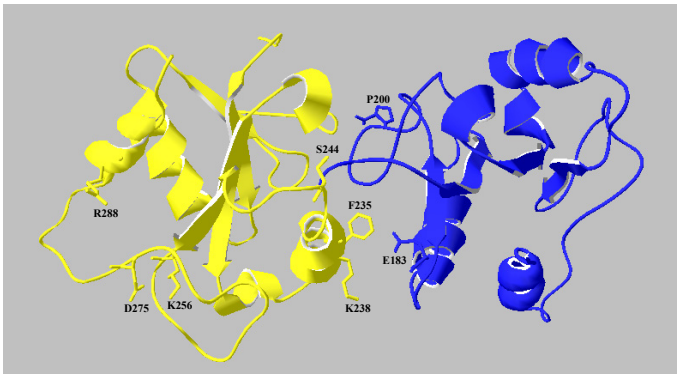

Figure 4

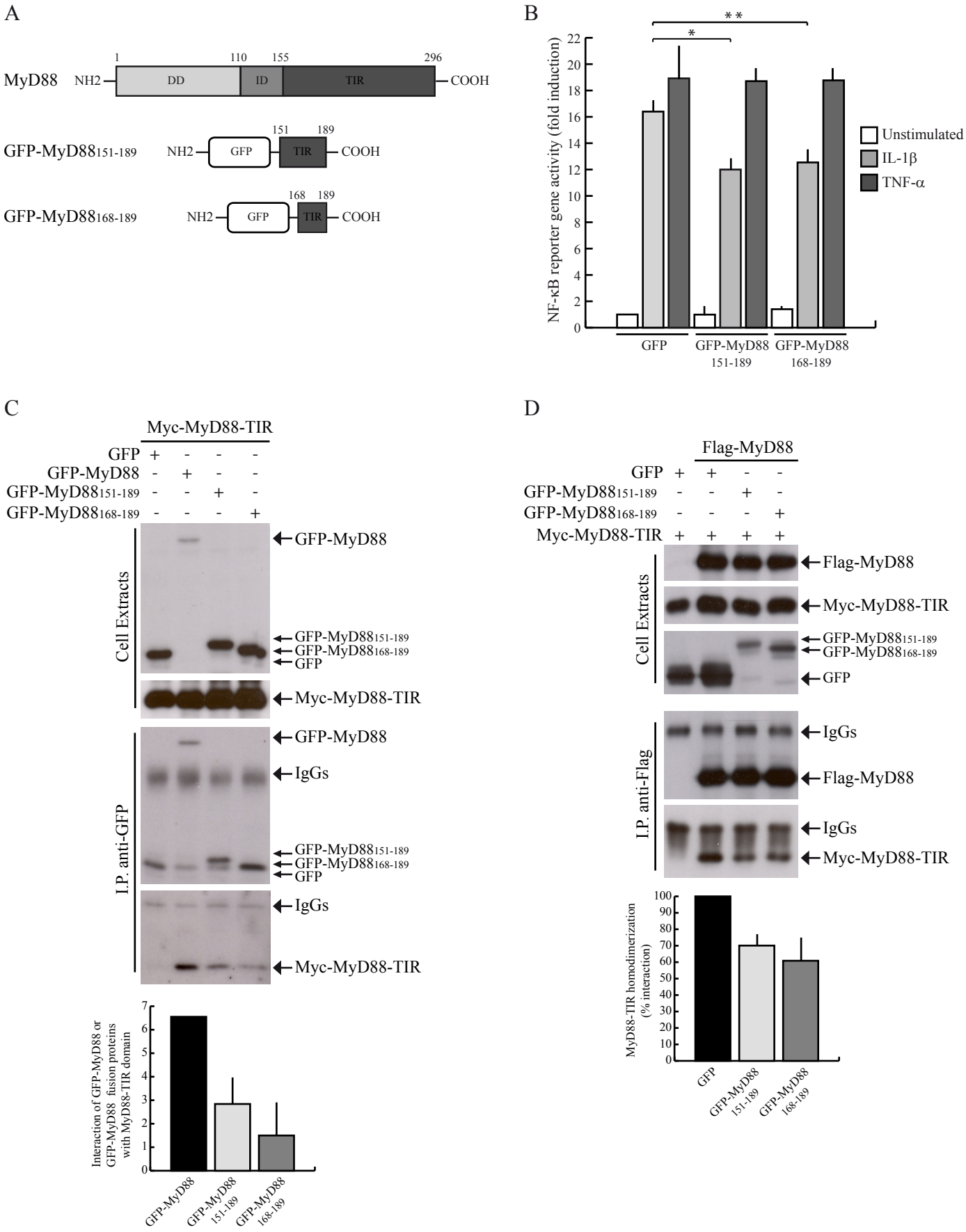
A
MyD88
NH2
DD
ID
TIR
COOH
1
110
155
296
GFP-MyD88151-189
GFP
151
189
GFP-MyD88168-189
168
B
NF-κB reporter gene activity (fold induction)
Unstimulated
IL-1β
TNF-α
GFP
GFP-MyD88 151-189
GFP-MyD88 168-189
C
Myc-MyD88-TIR
GFP-MyD88
GFP-MyD88151-189
GFP-MyD88168-189
Cell Extracts
Myc-MyD88-TIR
I.P. anti-GFP
IgGs
Interaction of GFP-MyD88 or GFP-MyD88 fusion proteins with MyD88-TIR domain
D
Flag-MyD88
Flag-MyD88
I.P. anti-Flag
MyD88-TIR homodimerization (% interaction)

Figure 5

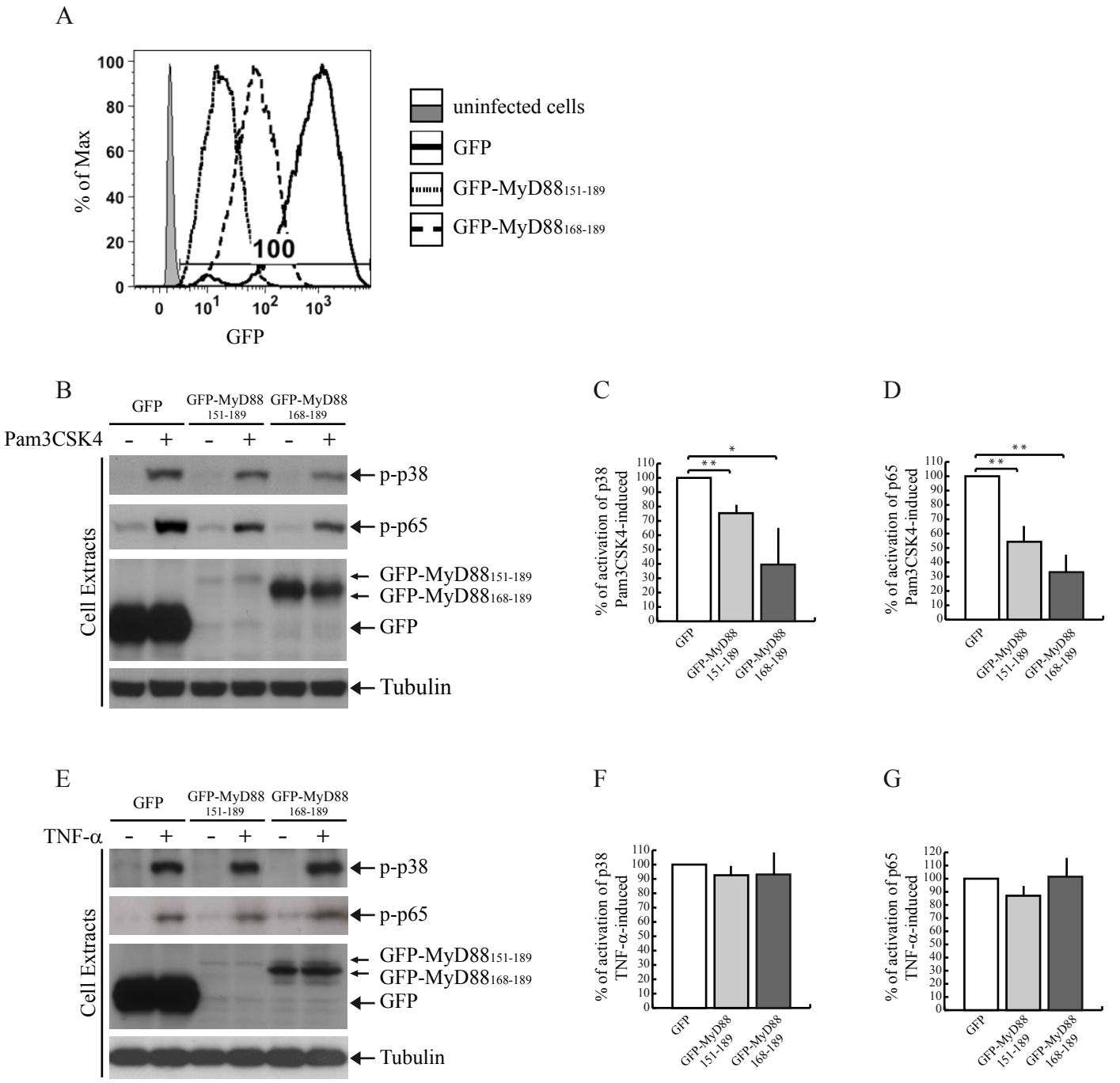
A
% of Max
GFP
100
uninfected cells
GFP
GFP-MyD88151-189
GFP-MyD88168-189
B
GFP
GFP-MyD88 151-189
GFP-MyD88 168-189
Pam3CSK4
Cell Extracts
p-p38
p-p65
GFP-MyD88151-189
GFP-MyD88168-189
GFP
Tubulin
C
% of activation of p38 Pam3CSK4-induced
D
% of activation of p65 Pam3CSK4-induced
E
TNF-α
F
% of activation of p38 TNF-α-induced
G
% of activation of p65 TNF-α-induced

Figure 6

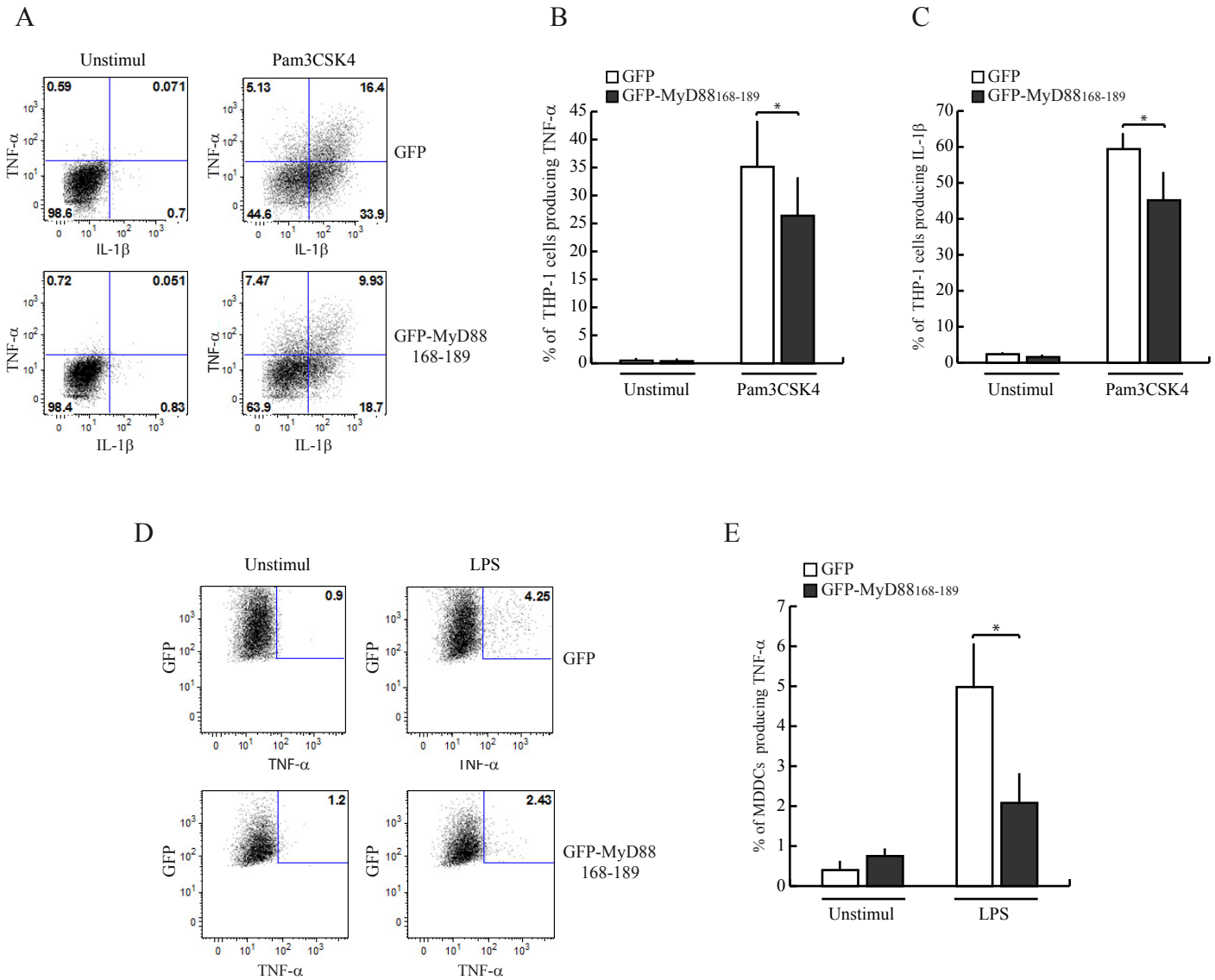
A
Unstimul
Pam3CSK4
0.59
0.071
98.6
0.7
5.13
16.4
44.6
33.9
GFP
0.72
0.051
98.4
0.83
7.47
9.93
63.9
18.7
GFP-MyD88
168-189
TNF-α
IL-1β
B
GFP
GFP-MyD88168-189
% of THP-1 cells producing TNF-α
Unstimul
Pam3CSK4
C
GFP
GFP-MyD88168-189
% of THP-1 cells producing IL-1β
Unstimul
Pam3CSK4
D
Unstimul
LPS
0.9
4.25
1.2
2.43
GFP
GFP-MyD88
168-189
TNF-α
E
GFP
GFP-MyD88168-189
% of MDDCs producing TNF-α
Unstimul
LPS

Figure 7